Influence of amino acid sequence in a peptidic Cu+-responsive luminescent probe inspired by the copper chaperone CusF.

A. Roux, M. Isaac, V. Chabert, S. A. Denisov, N. D. Mcclenaghan, O. Sénèque

Journal Name

ARTICLE

Influence of Amino Acid Sequence in a Peptidic Cu^{+}-Responsive Luminescent Probe Inspired by the Copper Chaperone CusF

Received 00th January 20xx,
Accepted 00th January 20xx

DOI: 10.1039/x0xx00000x

www.rsc.org/

A. Roux[†,a] M. Isaac[†,a] V. Chabert,[a] S. A. Denisov,[b] N. D. McClenaghan*[b] and O. Sénèque*[a]

Copper(I) is a soft metal ion that plays an essential role in living organisms and Cu^{+}-responsive probes are required to detect Cu^{+} ions in physiological conditions and understand its homeostasis as well as the diseases associated with its misregulation. In this article, we describe a series of cyclic peptides, which are structurally related to the copper chaperone CusF, and that behave as Cu^{+}-repsonsive probes. These peptide probes comprise the 16-amino acid loop of CusF cyclized by a β-turn inducer dipeptide and functionalized by a Tb^{3+} complex for its luminescence properties. The mechanism of luminescence enhancement relies on the modulation of the antenna effect between a tryptophan residue and the Tb^{3+} ion within the probe when Cu^{+} forms a cation-π interaction with the tryptophan. Here, we investigate the influence of the amino acid sequence of these cyclic peptides on the copper-induced modulation of Tb^{3+} emission and show that the rigid β-turn inducer Aib-D-Pro and insertion of the Tb^{3+} complex close to its tryptophan antenna are required to obtain turn-on Cu^{+} responsive probes. We also show that the amino acid sequence, especially the number and position of proline residues has a significant impact on metal-induced luminescence enhancement and metal-binding constant of the probes.

Introduction

Copper plays a crucial role in living organisms, in which it serves as a cofactor for several redox enzymes like oxidases or electron transfer proteins.[1,2] The most common oxidation states in biological systems are +I and +II but in the reducing cellular environment, mobile copper is mainly in the +I oxidation state. However, since free Cu^{+} can react with oxygen to yield superoxide ($O_2^{\bullet-}$), the first step in the generation of an oxidative stress, it is continually managed by proteins and its homeostasis is finely regulated.[3,4] Deregulation of copper homeostasis is often associated with severe diseases such as the Wilson[5] or Menkes[6] diseases, or possibly neurodegenerative diseases.[7] In order to better understand the biology of copper, several synthetic fluorescent probes for Cu^{+} as well as genetically encoded protein sensors have been designed.[8–10] Most of the synthetic probes operate on the basis of a photoinduced electron transfer (PET) switching mechanism, in which PET quenching of an excited fluorophore by a metal binding unit is blocked by metal binding. Genetically encoded sensors rely on modulation of fluorescence emission by conformational changes promoted by the metal ion using Förster resonance energy transfer (FRET).

We are developing luminescent probes for the detection of various bio-analytes, either metal cations[11–13] or biomolecules.[14] These probes are based (i) on binding domains of proteins (metal binding sites or biomolecule-binding domains) to benefit from their unparalleled recognition properties (selectivity for the target bio-analyte, dissociation constant in the suitable range for potential *in vivo* use, rapid dynamics of bio-analyte binding and dissociation) and (ii) on lanthanide(III) (Ln^{3+}) complexes as emitters in order to benefit from the desirable luminescence properties of Ln^{3+} ions. Indeed, most Ln^{3+} ions are luminescent with very interesting properties for biological applications: atom-like sharp emission bands at fixed wavelength depending on the Ln^{3+} cation (each Ln^{3+} having a fingerprint emission spectrum), low or no tendency to photobleaching and long luminescence lifetimes (in the µs to ms range), which allows time-gated detection to suppress background contribution of the biological medium (lifetime in the ns range).[15–23] However, direct absorption of Ln^{3+} ions is rather inefficient due to very low extinction coefficients (*ca.* 0.1-10 M^{-1} cm^{-1}) but indirect excitation of Ln^{3+} ion is possible through the so-called antenna effect, using a proximal chromophore that can absorb light and transfer its energy to the excited state of the Ln^{3+} cation.[24] Such a chromophore is deemed an antenna. A general strategy to create a responsive probe consists in modulating the efficiency of the antenna effect, i.e. Ln^{3+} sensitization, by an analyte. This can be achieved (i) by modulation of the distance between the antenna and the Ln^{3+} ion or (ii) by modulation of the photophysical properties of the antenna (by intramolecular charge transfer or PET mechanism for instance or by chemical reaction).[18,19,25–30] Another successful strategy for the design of lanthanide-based responsive probes is the modulation of the Ln^{3+} coordination

[a] Univ. Grenoble Alpes, CNRS, CEA, BIG, LCBM (UMR 5249), 38000 Grenoble, France. E-mail: olivier.seneque@cea.fr
[b] Univ. Bordeaux, CNRS, ISM (UMR 5255), 33405 Talence, France. E-mail: nathan.mcclenaghan@u-bordeaux.fr
† These authors contributed equally to this work.
Electronic Supplementary Information (ESI) available: synthesis of the peptides, luminescence characterizations and determination of the binding constants. See DOI: 10.1039/x0xx00000x

sphere, especially the number of coordinated water molecules (*q*), in order to change Ln^{3+} emission through modulation of the non-radiative deactivation of the excited Ln^{3+} ion.[31,19,25,28,30]

We have recently described a Cu^{+}-responsive luminescent probe, named $LCC1^{Tb}$,[11] demonstrating an original mechanism of antenna effect modulation, which differs from PET or FRET switching generally engineered in Cu^{+}-responsive probes.[8–10] This probe is inspired from the copper-chaperone CusF, a copper-trafficking protein encountered in the periplasm of gram negative bacteria,[32–35] and comprises a terbium complex conjugated to a cyclic peptide. The establishment of a cation-π interaction between a tryptophan side chain and the copper ion plays a crucial role in the turn-on behaviour of this luminescent probe (*vide infra*). In this article, we describe several cyclic peptides that were synthesized during our search for a Cu^{+}-responsive probe inspired by the CusF binding site, which led to $LCC1^{Tb}$. Throughout this article, we discuss the influence of the amino acid sequence on the copper-sensing properties of these peptides in relation with the establishment of the cation-π interaction.

Results and discussion

Previously reported $LCC1^{Tb}$: structure and mechanism

For the sake of clarity, this section contains details regarding the structure and the mechanism of $LCC1^{Tb}$ that were previously published[11] but that are essential to understand the behaviour of the new molecules presented in the current article.

The copper-chaperone CusF, which served as a basis for the design of $LCC1^{Tb}$, binds Cu^{+} selectively using a set of four amino acids located in a bent 16-amino acid β-hairpin loop: two methionines (Met/M), one histidine (His/H) and one tryptophan (Trp/W), whose aromatic side chain forms a cation-π interaction with the Cu^{+} ion (Fig. 1A). $LCC1^{Tb}$ (Fig. 1B) is a 18-amino acid cyclic peptide comprising a copper-binding loop derived from CusF and an Aib-D-Pro dipeptide to cyclize the loop (Aib = aminoisobutyric acid). Aib-D-Pro is an obligatory type-I' β-turn forming segment used to favour the formation of a β-sheet into the binding loop as in CusF (Fig. 1B).[36] As an emitting moiety, we chose a DOTA[Tb] chelate, which was grafted onto a side chain close to the tryptophan (Fig. 1B). The latter is a good antenna to sensitize Tb^{3+} luminescence.

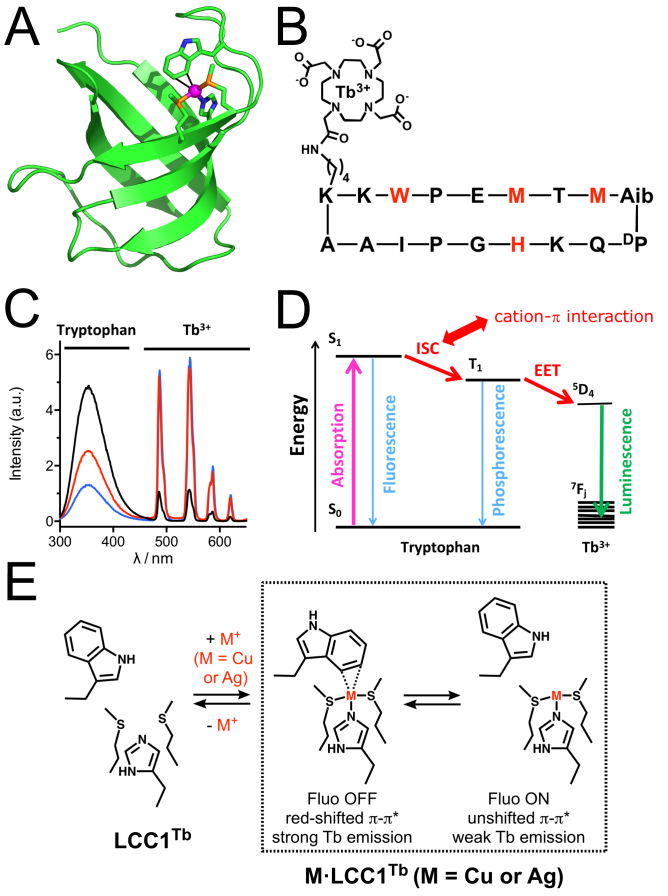

Fig. 1 (A) Crystallographic structure of CusF (pdb 2VB2[33]) showing the copper binding site. (B) Amino acid sequence of $LCC1^{Tb}$, chelating moieties in red. (C) Luminescence emission spectra (λ_{ex} = 280 nm) of $LCC1^{Tb}$ (black), $Cu{\cdot}LCC1^{Tb}$ (red) and $Ag{\cdot}LCC1^{Tb}$ (blue) in a degased HEPES buffer (10 mM, pH 7.5). (D) Simplified Jablonski-Perrin diagram of $LCC1^{Tb}$ and pertinent photophysical processes (ISC = intersystem crossing, EET = electronic energy transfer). (E) Metal binding equilibrium showing the two forms of the $M{\cdot}LCC1^{Tb}$ complex (M^{+} = Ag^{+} or Cu^{+}).

In buffered water solutions, $LCC1^{Tb}$ forms of a 1:1 complex with Cu^{+} but it is not able to bind any other physiological metal cations (Na^{+}, K^{+}, Mg^{2+}, Ca^{2+}, Mn^{2+}, Fe^{2+}, Co^{2+}, Ni^{2+}, Cu^{2+} and Zn^{2+}) due its thioether-containing coordination set, which can only bind soft metal cations. Cu^{+} binding results in a 6.1-fold increase of the sensitized Tb^{3+} emission (Fig. 1C). Additionally, $LCC1^{Tb}$ and CusF share spectral features characteristic of the establishment of a cation-π interaction between the Cu^{+} ion and the tryptophan indole, which includes a red-shift of the tryptophan π-π* transition and a quench of the tryptophan fluorescence (53% and 98% quench for $LCC1^{Tb}$ and CusF, respectively). Metal cation-π interactions are known to efficiently enhance intersystem crossing (ISC), which increases the population of the excited triplet state of the fluorophore, thereby quenching its fluorescence.[37] A detailed study relying on both steady-state and time-resolved (from ns to ms timescale) emission spectroscopy has revealed the following interesting features concerning $LCC1^{Tb}$.

(i) An enhancement of the tryptophan excited triplet state population is observed in the presence of Cu^{+}.

(ii) The terbium $^5D_4$ excited state is populated by electronic energy transfer from the tryptophan excited triplet state.

(iii) The Cu·LCC1^{Tb} complex exists in two different forms in equilibrium: one with the tryptophan forming the cation-π interaction and the other without the cation-π interaction (Fig. 1E). The former has a red-shifted π-π* transition, is not fluorescent and shows intense sensitized terbium emission whereas the latter has an unshifted π-π* transition, is fluorescent and shows weak terbium emission.

(iv) The cation-π interaction lowers the energy of the tryptophan excited triplet state by *ca.* 2300 cm^{-1}.

Hence, we can consider that in this system the mechanism for Cu$^+$-responsive turn-on terbium emission is the following: the binding of Cu$^+$ to LCC1^{Tb} results in the establishment of a copper-tryptophan cation-π interaction that enhances ISC, leading to an increased population of the tryptophan excited triplet state and, consequently, to enhanced energy transfer to the Tb^{3+} $^5D_4$ excited state, which emits more light (Fig. 1D).

In addition to Cu$^+$, LCC1^{Tb} is also able to bind the non-physiological cation Ag$^+$, as does CusF. Indeed, these two cations have very similar coordination properties. The spectroscopic behaviour of LCC1^{Tb} is similar with both Cu$^+$ and Ag$^+$ including the same metal-induced enhancement factor for terbium emission (Fig. 1C). The main differences are a greater extent of fluorescence quenching in the case of Ag$^+$ (78%) and a lowering of tryptophan excited triplet state of *ca.* 500 cm^{-1} instead of 2300 cm^{-1}.

Probe design: first attempts

Initial attempts to model the binding site of CusF used linear peptides incorporating the M_2HW coordination set, but these peptides precipitated in the presence of Cu$^+$ or Ag$^+$. Suspecting the formation of aggregates, we sought to restrict conformational freedom using a cyclic peptide for more precise control of the nuclearity and stoichiometry of the complex, with the expectation to favour the formation of 1:1 species. The sequence of the copper-binding loop of *E. coli* CusF is I^{34}HHDPIAAVNWPEMTM^{49} (coordinating amino acids are underlined). Besides the four coordinating amino acids H, W, M and M at positions 36, 44, 47 and 49, respectively, several amino acids might be important for the proper folding of the metal binding site and the establishment of the cation-π interaction. The crystal structure of *E. Coli* CusF[33] (Fig. 1B) shows that this loop is folded into a β-hairpin that is bent at the level of the two prolines facing each other. Since proline is usually not encountered in β-strands, we reasoned that these two prolines are important for the bending of the β-hairpin, which allows interaction between the tryptophan side chain and the copper ion. Several hydrophobic contacts are also observed between the side chains of the coordinating histidine (H^{36}) and tryptophan (W^{44}), the valine (V^{42}) and the second isoleucine (I^{39}) of the loop. Sequence alignment of CusF homologues shows that valine, isoleucine or leucine residues with alkyl side chains are always encountered at positions 39 and 42.[32] Therefore, V^{42} and I^{39} were considered important. A first cyclic peptide, LCC0(^{D}P-P)^{Tb} (Fig. 2), was designed as a model of the CusF binding loop. It comprises 18 amino acids including the important amino acids of the CusF binding loop as well as a D-Pro-L-Pro dipeptide to close the ring. Robinson *et al.* have shown that this dipeptide is an excellent template to induce the formation of β-hairpins in cyclic peptides that reproduce the conformation of natural β-hairpins in proteins.[38–41] We have already successfully used this template in the design of cyclic peptide-based models of zinc finger sites presenting β-hairpins.[42–44] Several supposedly non essential amino acids of the CusF binding loop were changed: (i) a glycine was needed for synthesis purposes to avoid epimerization during cyclization and it was introduced in place of D^{37}; (ii) H^{35} and N^{43} were replaced by lysines to provide positively charged amino acids to ensure solubility of the peptide and (iii) I^{34} was changed for a lysine to take advantage of its amino side chain to easily graft the DOTA ligand. This position was chosen to insert the Tb^{3+} complex in order to preserve, as far as possible, the CusF binding loop sequence in this first model. The synthesis of LCC0(^{D}P-P)^{Tb} and other peptides is described in the ESI.

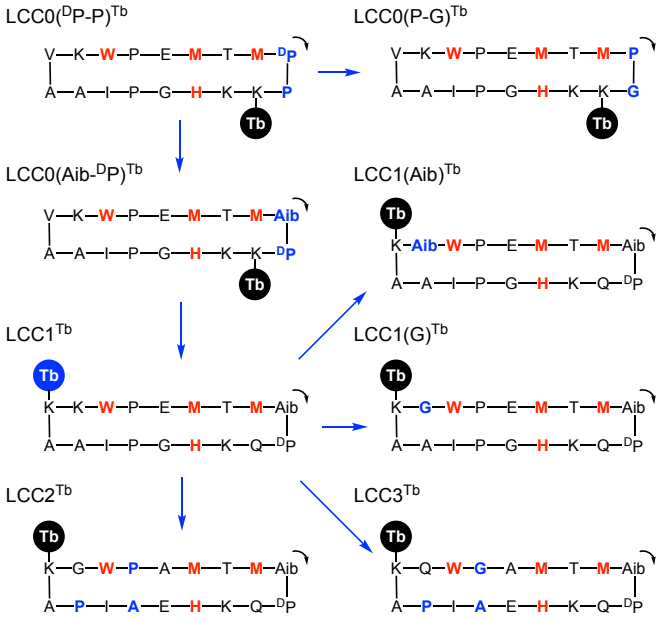

Fig. 2 Cyclic peptides used in this study. Coordinating amino acids are shown in red. Major changes from one peptide to the other are shown in blue.

The metal binding properties of this peptide were investigated with Ag$^+$ and Cu$^+$ in degassed HEPES buffer (10 mM, pH 7.5). Indeed, all peptides presented throughout this article behave in a similar way with Ag$^+$ or Cu$^+$ as previously observed for LCC1^{Tb}. The titration of LCC0(^{D}P-P)^{Tb} by Ag$^+$ in HEPES buffer monitored by tryptophan fluorescence (λ_{ex} = 280 nm) shows a quenching of the tryptophan emission upon addition of Ag$^+$ with a plateau above 1 eq. of added metal cation, attesting to the formation of a 1:1 complex (Fig. 3A). In addition to the tryptophan fluorescence quench (44%), a slight red-shift of the π-π* transition (*ca.* 2 nm) is observed upon formation of the Ag·LCC0(^{D}P-P)^{Tb} complex (Fig. 3B). These two features are indicative of the establishment of the cation-π interaction but they are rather weak in intensity compared to CusF (98% fluorescence quench and *ca.* 12 nm-shift of the π-π* transition

as evaluated at the half-height of the band). A similar behaviour is observed with Cu^{+}. Concerning the sensitized terbium emission in degassed solutions, addition of Ag^{+} leads to a small increase of Tb^{3+} emission (10%) whereas a 60% decrease is observed with Cu^{+} (Fig. 3C). The excitation spectra for tryptophan fluorescence (λ_{em} = 357 nm) and terbium emission (λ_{em} = 545 nm) were also recorded (Fig. S2 of ESI). Interestingly, the terbium emission excitation spectra of the Ag^{+} and Cu^{+} complexes are shifted with respect to the free peptide whereas those of fluorescence emission are not. This has been described previously for $LCC1^{Tb}$. It reveals that two species are in equilibrium for the complexes: one with a tryptophan forming the cation-π interaction (with red-shifted π-π* transition absorption, non fluorescent tryptophan and emissive terbium) and one without cation-π interaction (with unshifted π-π* transition absorption, fluorescent tryptophan and weakly emissive terbium) as depicted in Fig. 1E.

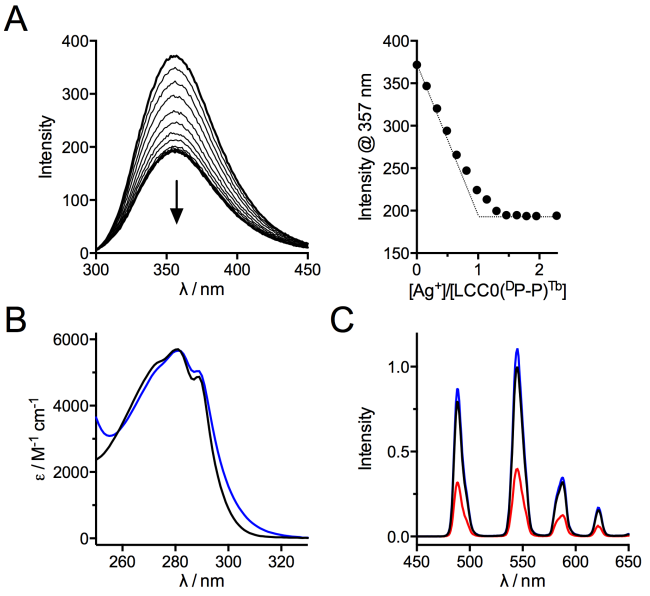

Fig. 3 (A) Fluorescence titration (λ_{ex} = 280 nm) of $LCC0(^{D}P\text{-}P)^{Tb}$ by Ag^{+} in HEPES buffer (10 mM, pH 7.5). (B) Electronic absorption spectra of $LCC0(^{D}P\text{-}P)^{Tb}$ (black) and $Ag{\cdot}LCC0(^{D}P\text{-}P)^{Tb}$ (blue). (C) Time-gated Tb^{3+} emission spectra (λ_{ex} = 280 nm, 200 µs delay time) of $LCC0(^{D}P\text{-}P)^{Tb}$ (black), $Ag{\cdot}LCC0(^{D}P\text{-}P)^{Tb}$ (blue) and $Cu{\cdot}LCC0(^{D}P\text{-}P)^{Tb}$ (red).

Influence of the cyclizing dipeptide

In order to assess the influence of the cyclizing dipeptide, we changed the D-Pro-L-Pro dipeptide for Aib-D-Pro or L-Pro-Gly dipeptides. D-Pro-L-Pro and Aib-D-Pro are two rigid turn templates that induce a β-sheet. D-Pro-L-Pro induces a flat β-sheet whereas the two β-strands are twisted in the case of Aib-D-Pro, as are those in proteins.[36] L-Pro-Gly is a less rigid dipeptide that is less prone to induce β-strands. The corresponding peptides, $LCC0(Aib\text{-}^{D}P)^{Tb}$ and $LCC0(P\text{-}G)^{Tb}$, bind 1 equivalent of Ag^{+} or Cu^{+} as does $LCC0(^{D}P\text{-}P)^{Tb}$. They behave mostly as $LCC0(^{D}P\text{-}P)^{Tb}$ but with some differences. For both peptides, a partial quenching of the tryptophan fluorescence and a red-shift of the π-π* transition are observed. However, compared to $LCC0(^{D}P\text{-}P)^{Tb}$, the quenching is higher for $LCC0(Aib\text{-}^{D}P)^{Tb}$ and lower for $LCC0(P\text{-}G)^{Tb}$ (Fig. 4A). The same trend is observed for the red-shift of the π-π* transition (Fig. 4B). This indicates a greater tendency to form the cation-π interaction for $LCC0(Aib\text{-}^{D}P)^{Tb}$ (the equilibrium in Fig. 1E is shifted toward the "Fluo OFF" form) compared to $LCC0(^{D}P\text{-}P)^{Tb}$ and a lower tendency for $LCC0(P\text{-}G)^{Tb}$. As for $LCC0(^{D}P\text{-}P)^{Tb}$, addition of Ag^{+} to $LCC0(Aib\text{-}^{D}P)^{Tb}$ led to a modest (5%) increase of Tb^{3+} emission whereas it led to a 17% quench in the case of $LCC0(P\text{-}G)^{Tb}$ (Fig. 5B). For both peptides, addition of Cu^{+} resulted in a lower Tb^{3+} emission (Fig. 5).

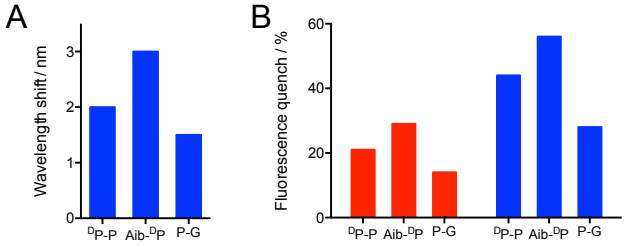

Fig. 4 Influence of the dipeptide template on spectroscopic features: (A) Comparison of the red-shift of the π-π* transition between Ag^{+} complexes of $LCC0(^{D}P\text{-}P)^{Tb}$, $LCC0(Aib\text{-}^{D}P)^{Tb}$ and $LCC0(P\text{-}G)^{Tb}$. (B) Comparison of the tryptophan fluorescence quench upon Ag^{+} (blue) or Cu^{+} (red) binding to peptides $LCC0(^{D}P\text{-}P)^{Tb}$, $LCC0(Aib\text{-}^{D}P)^{Tb}$ and $LCC0(P\text{-}G)^{Tb}$.

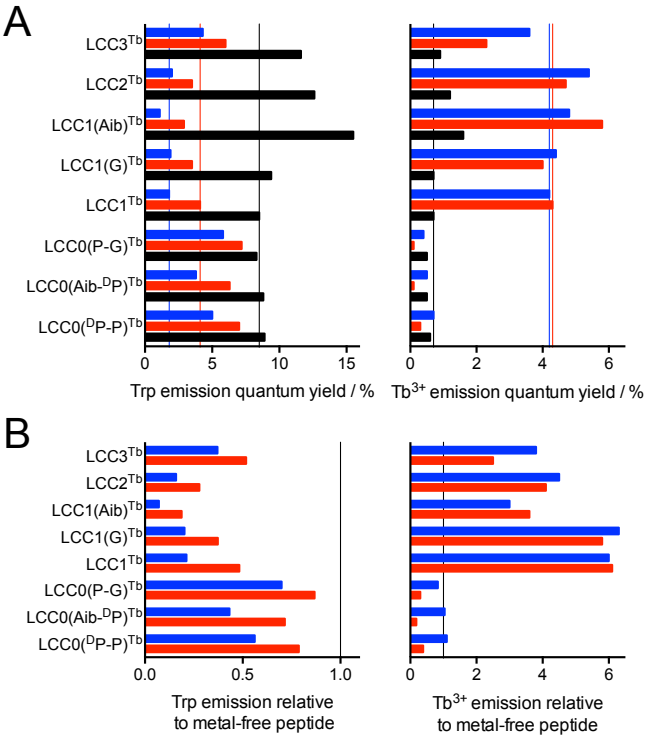

Fig. 5 (A) Quantum yields (λ_{ex} = 280 nm) of tryptophan fluorescence emission (*left*) and terbium luminescence emission (*right*) for metal-free (black), Cu^{+}-bound (red) and Ag^{+}-bound (blue) peptides determined by comparison with $LCC1^{Tb}$ in anaerobic conditions.[11] Solid black, red and blue lines correspond to the emission of $LCC1^{Tb}$ and its complexes, for comparison purpose. (B) Tryptophan (*left*) and terbium (*right*) emission intensity of Cu^{+}-bound (red) and Ag^{+}-bound (blue) relative to metal-free peptide. The black solid line corresponds to the emission of the metal-free peptide normalized to 1.

The conformation of peptides was examined by circular dichroism (CD). The CD spectra of $LCC0(^{D}P\text{-}P)^{Tb}$ and $LCC0(Aib\text{-}^{D}P)^{Tb}$ present a strong negative signal at 200 nm (Fig. 6A,B). They

are characteristic of peptides with an undefined conformation (random coil). Addition of Ag^+ to LCC0(^{D}P-P)^{Tb} leads to a less negative CD signal at 200 nm with a marked shoulder at 223 nm and small positive band at 240 nm (ESI). These features are more pronounced for Ag·LCC0(Aib-^{D}P)^{Tb} with a much reduced negative ellipticity at 200 nm, two positive bands at 208 nm and 240 nm and a negative band at 223 nm. This indicates a better propensity of LCC0(Aib-^{D}P)^{Tb} to fold upon metal binding. In order to gain more insight into the conformational behaviour, LCC0(Aib-^{D}P)^{La}, the diamagnetic analogue of LCC0(Aib-^{D}P)^{Tb} with lanthanum replacing terbium, was prepared and analysed by ^{1}H NMR. Its spectrum in H_2O/D_2O showed broad resonances in agreement with conformational motions. In the presence of Ag^+ (1.0 eq.), the NMR signals become even broader attesting again to the conformational flexibility of the silver complexes. Interestingly, several peaks were observed for the tryptophan indole NH resonance around 10 ppm in agreement with the co-existence of complexes with bound and unbound tryptophan deduced from photophysical studies. Finally, the apparent Ag^+ binding constants K of the three LCC0 peptides (K = [Ag·LCC0^{Tb}]/([Ag^+][LCC0^{Tb}])) were measured using imidazole as a competitor (Table 1 and ESI).[45] LCC0(P-G)^{Tb} shows the lowest affinity among the three LCC0 peptides. Overall, among D-Pro-L-Pro, L-Pro-Gly and Aib-D-Pro dipeptide templates, the latter seems to be the best suited to combine the best ability to establish the cation-π interaction and to form the tightest complexes.

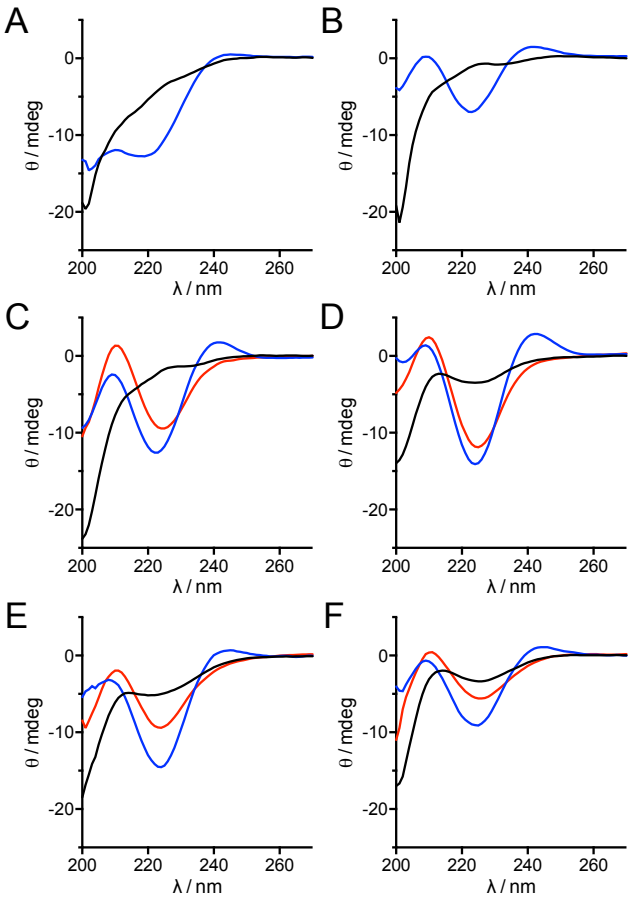

Fig. 6 CD spectra of solutions of (A) LCC0(^{D}P-P)^{Tb}, (B) LCC0(Aib-^{D}P)^{Tb}, (C) LCC1^{Tb}, (D) LCC1(Aib)^{Tb}, (E) LCC2^{Tb} and (F) LCC3^{Tb} (20 μM) in phosphate buffer (20 mM, pH 7) in their metal-free (black), Cu^+-bound (red) and Ag^+-bound (blue) forms.

Table 1 Cu^+ and Ag^+ binding constants K (in M^{-1}) at pH 7.5 for the peptides used in this study, determined by competition experiments with imidazole (nd = not determined).

	log K (± 0.2)	
Peptide	Cu^+	Ag^+
LCC0(^{D}P-P)^{Tb}	nd	6.8
LCC0(Aib-^{D}P)^{Tb}	nd	6.8
LCC0(P-G)^{Tb}	nd	5.7
LCC1^{Tb}	9.4[a]	7.3[a]
LCC1(G)^{Tb}	9.9	8.0
LCC1(Aib)^{Tb}	10.3	8.8
LCC2^{Tb}	10.2	8.0
LCC3^{Tb}	9.2	7.2

[a] Data taken from reference 11.

Influence of the lanthanide chelate position

Within the LCC0 peptide family, the DOTA[Tb] complex is quite remote from its tryptophan antenna. Reasoning that the distance between the terbium complex and the tryptophan antenna could be an issue for the terbium sensitization process and the luminescence response of the probe, the DOTA[Tb] complex was grafted closer to the tryptophan. The crystal structure of CusF shows hydrophobic contacts between the tryptophan indole and the alkyl side-chains of Val42.[33] Having reasoned that the four-carbon side chain of a lysine could establish similar contacts, valine was substituted by a lysine with an appended DOTA ligand. Aib-D-Pro was selected as a cyclizing dipeptide and a glutamine was introduced next to the D-Pro. This led to peptide LCC1^{Tb} (Fig. 1 and 2).[11] Regarding structural aspects, the CD spectra of LCC1^{Tb} and its metal complexes (Fig. 6) are reminiscent of those of LCC0(Aib-^{D}P)^{Tb} with a random coil signature in the absence of cation and bands at 208 nm (+), 223 nm (–) and 240 nm (+) for the silver complex. The copper complex displays the same bands at 208 nm (+) and 223 nm (–) but not the band at 240 nm. Compared to LCC0(Aib-^{D}P)^{Tb}, the tryptophan emission of LCC1^{Tb} is similar in the absence of metal cation but lower in the presence of both Cu^+ and Ag^+ cations (Fig. 5). The greater quenching of tryptophan emission observed in the presence of the cations parallels the bigger red-shift of the π-π* band (5 nm *vs* 3 nm for Ag^+) indicating a greater tendency to establish the cation-π interaction in the case of LCC1^{Tb}. This may be ascribed to the valine-to-lysine mutation that would favour the tryptophan-bound forms of the copper or silver complexes. Displacing the Tb^{3+} complex has also a major effect (i) on the terbium emission quantum yield, which is higher for both the metal-free and the metal-bound probe when the Tb^{3+} ion closer to the tryptophan antenna, and (ii) on the probe response with a *ca.* 6-fold increase of terbium emission upon Cu^+ or Ag^+ binding for LCC1^{Tb}, resulting in an interesting turn-on response for both Cu^+ and Ag^+ (Fig. 5B) as described in a previous communication[11] and as summarized in the introduction. In addition to favouring the cation-π position compared to peptides of the LCC0 family, changing the position of the lysine-DOTA residue slightly increases the affinity for Cu^+ and Ag^+ (Table 1).

Influence of the binding loop sequence

Our next investigations were directed towards the amino acids that compose the binding loop. Firstly, when looking at the Ramachandran plot[46,47] of the crystal structure of CusF, we noticed that asparagine 43 (Asn43) of the copper-binding loop has backbone dihedral angles φ and ψ[‡] values of + 60° and + 44°, respectively, which lies in the sparsely populated left-handed α-helix region of the Ramachandran plot. These values are rarely encountered for L-amino acids because of steric clashes arising between the main chain and the side chain but more frequently for glycine, which is achiral and has no side chain. Interestingly, several CusF homologues feature a glycine at position 43.[32] Therefore, we decided to assess the influence of having a glycine or an Aib residue, which is also non-chiral but restricts more than glycine the conformational space, at this position (N-side of tryptophan) in LCC1^{Tb}. For this purpose, peptides LCC1(G)^{Tb} and LCC1(Aib)^{Tb} (Fig. 2) were synthesized and analysed. Both peptides are able to establish the cation-π interaction as demonstrated by characteristic features mentioned above and both show turn-on sensitized terbium emission upon metal binding (Fig. 5B). The emission properties of LCC1(G)^{Tb} are almost identical to those of LCC1^{Tb} (Fig. 5A), indicating that the Asn-to-Gly mutation has limited impact. The only noticeable difference is a higher binding constant for LCC1(G)^{Tb} compared to LCC1^{Tb} (Δlog *K* = 0.5 and 0.7 for Cu^+ and Ag^+, respectively; Table 1). More differences are observed between LCC1^{Tb} and LCC1(Aib)^{Tb}. The latter displays a slightly higher red-shift of the π-π* absorption (6 nm *vs* 5 nm), a higher tryptophan emission in the free form and a lower one in the metal-bound form, which gives a greater quenching of tryptophan emission upon metal binding, and higher sensitized terbium emission in both the free and metal-bound forms (Fig. 5). Unfortunately, this translates into a lower metal-induced enhancement of sensitized terbium emission (3.6- and 3.0-fold for Cu^+ and Ag^+, respectively, in the case of LCC1(Aib)^{Tb} compared to 6.1- and 6.0-fold for LCC1^{Tb}, in anaerobic conditions; Fig. 5B). Nevertheless, LCC1(Aib)^{Tb} forms significantly more stable complexes than LCC1^{Tb} (Δlog *K* = 0.9 and 1.5 for Cu^+ and Ag^+, respectively; Table 1). CD provides some clues to explain this behaviour. The CD spectra of the metal-free form is less negative at 200 nm for LCC1(Aib)^{Tb} compared to LCC1^{Tb} and a negative band at 223 nm is clearly observed in the spectrum of the Aib variant, which is not observed in the parent probe (Fig. 6C,D). The spectra of the metal-bound forms show the bands at 208 nm (+), 223 nm (–) and 240 nm (+, Ag^+ only) but they are slightly more intense in the case of the Aib variant. Altogether, the Asn-to-Aib mutation seems to limit conformational motions of the peptide and to stabilize a certain fold. This is beneficial to metal affinities and emission quantum yields but detrimental to the probe response, mainly because of higher emission of terbium in the free form. The Aib residue, by rigidifying the cyclic peptide scaffold may lower non-radiative deactivation of tryptophan resulting in a higher fluorescence emission and in a more efficient Tb^{3+} sensitization. This effect may be more pronounced in the metal-free form than in the metal-bound form where the metal ion contributes to the rigidification of the scaffold also.

By looking at the sequence alignment of CusF homologues,[32] we noticed that the two prolines of the metal binding loop are not always at the same position and in some cases, one of them is missing. Indeed, some homologues have a proline in position 40 instead of 38 and others have only a single proline either at position 40 or 45. Therefore, starting from LCC1^{Tb}, we implemented the sequence of the Cu-binding loop of *Klebsiella pneumonia* CusF,[32] with two prolines at positions 40 and 45, and that of *Cupriavidus metallidurans* CH34 C-terminal domain of SilB,[48] with a single proline at position 40, into the cyclic peptide to give LCC2^{Tb} and LCC3^{Tb} probes, respectively (Fig. 2). Both LCC2^{Tb} and LCC3^{Tb} form 1:1 complexes with Ag^+ and Cu^+ and behave as turn-on emission probes regarding terbium emission (Fig. 5B), as does the parent probe LCC1^{Tb}. However, the red-shift of the π-π* absorption upon Ag^+ binding is lower (4 nm) in the case of LCC3^{Tb} compared to LCC1^{Tb} and LCC2^{Tb} (5 nm), suggesting a lower capacity to establish the cation-π interaction. The quantum yield of tryptophan emission is higher for metal-free LCC2^{Tb} and LCC3^{Tb} than for LCC1^{Tb} (Fig. 4). As for the Aib variant of LCC1^{Tb}, this goes along with a more structured peptide as deduced from comparison of CD spectra, which shows a negative band at 220 nm for both metal-free LCC2^{Tb} and LCC3^{Tb} (Fig. 6E,F). Additionally, the terbium emission of those metal-free peptides is higher than that of LCC1^{Tb}, as is the Aib variant. In the Cu^+- or Ag^+-bound forms, LCC2^{Tb} has a similar tryptophan quantum yield as LCC1^{Tb} but that of LCC3^{Tb} is higher

Table 2 Summary of life times measured by time resolved emission spectroscopy.

Compound[a]	Tryptophan fluorescence decay / ns (± 0.2 ns)	Tryptophan phosphorescence decay / µs (± 2 µs)	Tb^{3+} luminescence rise / µs (± 2 µs)	Tb^{3+} luminescence decay / ms (± 0.01 ms)
LCC1^{Tb}	0.9 (13 %), 4.8 (87 %)	not detected	23	1.98
Cu·LCC1^{Tb}	0.7 (16 %), 3.9 (84 %)	16	16	1.90
Ag·LCC1^{Tb}	0.9 (17 %), 4.2 (83 %)	19	18	1.95
LCC2^{Tb}	1.0 (10 %), 4.8 (90 %)	not detected	17	1.97
Cu·LCC2^{Tb}	0.7 (17 %), 4.1 (83 %)	13	14	1.93
Ag·LCC2^{Tb}	1.1 (18 %), 4.6 (82 %)	18	22	1.96
LCC3^{Tb}	0.9 (9 %), 4.2 (91 %)	not detected	19	1.99
Cu·LCC3^{Tb}	0.7 (12 %), 3.8 (88 %)	14	15	1.93
Ag·LCC3^{Tb}	1.1 (13 %), 4.1 (87 %)	23	23	1.97

[a] Data for LCC1^{Tb} are taken from reference 11.

(Fig. 4). Together with the lower red-shift of the π-π* absorption of the latter, this suggests that LCC3^{Tb} has a lower tendency to form the cation-π interaction compared to LCC1^{Tb} and LCC2^{Tb}. Indeed, the molar fraction of complex with metal-bound tryptophan seems to be higher for peptides with two prolines than those with a single proline. The consequence is a lower terbium emission of the metal-bound species in the case of the peptide with a single proline compared to the two-proline probes. Altogether, although responding to Cu^+ or Ag^+, LCC2^{Tb} and LCC3^{Tb} present a less significant metal-induced enhancement of terbium emission than LCC1^{Tb} (Fig. 5B, 4.1-, 2.5- and 6.1-fold, respectively, in the case of Cu^+ and 4.5-, 3.8- and 6.0-fold in the case of Ag^+). Regarding binding constants, LCC3^{Tb} has the same affinity for Cu^+ and Ag^+ as LCC1^{Tb} whereas LCC2^{Tb} forms more stable complexes ($\Delta\log K$ = 0.8 and 0.7 for Cu^+ and Ag^+, respectively; Table 1). Finally, LCC2^{Tb} and LCC3^{Tb} were studied by time-resolved emission spectroscopy. Tryptophan fluorescence was observed on the ns time-scale. In both the metal-free and Ag^+-bound forms, the fluorescence decay is bi-exponential with a short lifetime around 0.9 ns and a longer one around 4.5 ns (Table 2). This is typical of tryptophan fluorescence and these values are similar to those determined for LCC1^{Tb}.[11] Terbium emission was observed in the time-gated mode on the μs and ms time scales. As for LCC1^{Tb}, the terbium emission rise time lies in the 15-25 ms range. Tryptophan phosphorescence, which could be observed in the case of the Cu^+ and Ag^+ complexes only, has a decay time of *ca.* 20 ms that matches the rise time of terbium emission within error (± 2 μs). This indicates that in the case of LCC2^{Tb} and LCC3^{Tb}, the sensitizing mechanism involves electronic energy transfer from the triplet excited state of tryptophan to the $^5D_4$ excited state of terbium, as previously observed for LCC1^{Tb}. The sensitization mechanism is thus not modified. To summarize, LCC1^{Tb}, LCC2^{Tb} and LCC3^{Tb} display turn-on terbium luminescence response to Cu^+ and Ag^+ and have very similar behaviour (Fig. 5). However, the single-proline variant (LCC3^{Tb}) displays lowered terbium luminescence modulation compared to the two-proline probes. For the two-proline probes, the position of the proline influences both luminescence response and binding constants.

Conclusions

In this article, we have investigated the influence of amino acid sequence in a family of bio-inspired Cu^+-responsive peptide probes. These probes are 18-amino acid cyclic peptides comprising the 16-amino acid copper-binding loop of the CusF protein, a periplasmic copper chaperone in gram-negative organisms. The loop is closed by a dipeptide turn. The copper-binding site is composed of two methionine thioethers, the imidazole ring of histidine and the indole ring of a tryptophan, which establishes a cation-π interaction with Cu^+ in CusF. A Tb^{3+} complex is grafted onto one of the amino acid side chains of the cyclic peptide to provide a luminescence reporter. In this system, the tryptophan amino acid serves as an antenna to sensitize Tb^{3+} luminescence. A key point in the design of turn-on probes in this system is to reproduce the cation-π interaction because it increases ISC within the tryptophan indole, thereby allowing more energy to be transferred to the $^5D_4$ Tb^{3+} excited state, resulting in an enhanced Tb^{3+} emission in the presence of Cu^+.[11] By studying this family of peptides, we have highlighted several factors that govern the cation-π interaction and thus, the behaviour of the probe. First, the ring-closing dipeptide plays a crucial role in the establishment of the cation-π interaction. Indeed, we found that a rigid β-turn inducer such as D-Pro-L-Pro or Aib-D-Pro is required, whereas a flexible one (e.g. Pro-Gly) is not suitable. However, Aib-D-Pro, which favours the formation of twisted β-sheets, is more efficient than D-Pro-L-Pro at forcing the interaction between the indole and the Cu^+ ion. The second requirement is to place the Tb^{3+} complex very close to its tryptophan antenna. Taking into account these two requirements, we have obtained several turn-on Cu^+- and Ag^+-responsive probes displaying variable luminescence quantum yields, metal-induced luminescence enhancement (ranging from 2.5 to 6.1 for Cu^+ and from 3 to 6 for Ag^+) and affinities (ranging from $10^{9.2}$ to $10^{10.3}$ M^{-1} for Cu^+ and $10^{7.2}$ to $10^{8.8}$ M^{-1} for Ag^+). We have shown that having two prolines in the metal-binding loop is better than a single proline, providing probes with higher luminescence enhancement and higher metal-binding constants. This highlights the influence of conformational flexibility within the cycle. Nevertheless, this cyclic peptide scaffold seems rather tolerant to amino acid sequence changes provided that the Aib-D-Pro dipeptide is used as a closing turn and that the Tb^{3+} complex is close to the tryptophan. Regarding the strength of the cation-π interaction that is superior in CusF compared to our probes, as judged by the red-shift of the π-π* transition (12 nm) and the almost complete quench of tryptophan fluorescence, we believe that there is still room to improve this system, by trying to preorganize the metal-free peptide into a conformation that is the same as the metal-bound form establishing the cation-π interaction as it is the case for CusF. Our efforts are now directed toward the replacement of the tryptophan indole by other aromatic antenna to sensitize luminescence of other Ln^{3+} and shift excitation and emission wavelength towards lower energy.

Conflicts of interest

There are no conflicts to declare.

Acknowledgements

OS acknowledge the Agence Nationale de la Recherche (ANR-12-BS07) and the Labex ARCANE (ANR-11-LABX-0003) for financial support.

Notes and references

‡ φ is defined by the backbone dihedral angle created by C_{i-1}–N_i–$C\alpha_i$–C_i along the peptide chain and ψ is defined by the dihedral angle created by N_i–$C\alpha_i$–C_i–N_{i+1}.

1 K. E. Vest, H. F. Hashemi and P. A. Cobine, in *Metallomics and the Cell*, ed. L. Banci, Springer Netherlands, 2013, pp. 451–478.
2 C. Rensing and S. F. McDevitt, in *Metallomics and the Cell*, ed. L. Banci, Springer Netherlands, 2013, pp. 417–450.
3 B.-E. Kim, T. Nevitt and D. J. Thiele, *Nat. Chem. Biol.*, 2008, **4**, 176–185.
4 S. Lutsenko, *Metallomics*, 2016, **8**, 840–852.
5 P. C. Bull, G. R. Thomas, J. M. Rommens, J. R. Forbes and D. W. Cox, *Nature Genet.*, 1993, **5**, 327–337.
6 C. Vulpe, B. Levinson, S. Whitney, S. Packman and J. Gitschier, *Nature Genet.*, 1993, **3**, 7–13.
7 J. A. Duce and A. I. Bush, *Prog. Neurobiol.*, 2010, **92**, 1–18.
8 C. J. Fahrni, *Curr. Opin. Chem. Biol.*, 2013, **17**, 656–662.
9 J. Joseph A. Cotruvo, A. T. Aron, K. M. Ramos-Torres and C. J. Chang, *Chem. Soc. Rev.*, 2015, **44**, 4400–4414.
10 K. P. Carter, A. M. Young and A. E. Palmer, *Chem. Rev.*, 2014, **114**, 4564–4601.
11 M. Isaac, S. A. Denisov, A. Roux, D. Imbert, G. Jonusauskas, N. D. McClenaghan and O. Sénèque, *Angew. Chem., Int. Ed.*, 2015, **54**, 11453–11456.
12 M. Isaac, L. Raibaut, C. Cepeda, A. Roux, D. Boturyn, S. V. Eliseeva, S. Petoud and O. Sénèque, *Chem. Eur. J.*, 2017, **23**, 10992–10996.
13 M. Isaac, A. Pallier, F. Szeremeta, P.-A. Bayle, L. Barantin, C. S. Bonnet and O. Sénèque, *Chem. Commun.*, DOI:10.1039/C8CC04366C.
14 L. Raibaut, W. Vasseur, G. D. Shimberg, C. Saint-Pierre, J.-L. Ravanat, S. L. J. Michel and O. Sénèque, *Chem. Sci.*, 2017, **8**, 1658–1664.
15 J.-C. G. Bünzli and S. V. Eliseeva, in *Lanthanide Luminescence*, eds. P. Hänninen and H. Härmä, Springer Berlin Heidelberg, 2011, pp. 1–45.
16 J.-C. G. Bünzli, *Chem. Rev.*, 2010, **110**, 2729–2755.
17 C. P. Montgomery, B. S. Murray, E. J. New, R. Pal and D. Parker, *Accounts Chem. Res.*, 2009, **42**, 925–937.
18 E. J. New, D. Parker, D. G. Smith and J. W. Walton, *Curr. Opin. Chem. Biol.*, 2010, **14**, 238–246.
19 M. C. Heffern, L. M. Matosziuk and T. J. Meade, *Chem. Rev.*, 2014, **114**, 4496–4539.
20 S. J. Butler, M. Delbianco, L. Lamarque, B. K. McMahon, E. R. Neil, R. Pal, D. Parker, J. W. Walton and J. M. Zwier, *Dalton Trans.*, 2015, **44**, 4791–4803.
21 A. J. Amoroso and S. J. A. Pope, *Chem. Soc. Rev.*, 2015, **44**, 4723–4742.
22 M. Sy, A. Nonat, N. Hildebrandt and L. J. Charbonnière, *Chem. Commun.*, 2016, **52**, 5080–5095.
23 I. Martinić, S. V. Eliseeva and S. Petoud, *J. Lumin.*, 2017, **189**, 19–43.
24 S. I. Weissman, *J. Chem. Phys.*, 1942, **10**, 214–217.
25 A. Thibon and V. C. Pierre, *Anal. Bioanal. Chem.*, 2009, **394**, 107–120.
26 E. Pazos and M. E. Vázquez, *Biotechnol. J.*, 2014, **9**, 241–252.
27 S. J. Bradberry, A. J. Savyasachi, M. Martinez-Calvo and T. Gunnlaugsson, *Coord. Chem. Rev.*, 2014, **273**–**274**, 226–241.
28 X. Wang, H. Chang, J. Xie, B. Zhao, B. Liu, S. Xu, W. Pei, N. Ren, L. Huang and W. Huang, *Coord. Chem. Rev.*, 2014, **273**–**274**, 201–212.
29 C. Zhao, Y. Sun, J. Ren and X. Qu, *Inorg. Chim. Acta*, 2016, **452**, 50–61.
30 S. Shuvaev, M. Starck and D. Parker, *Chem. Eur. J.*, 2017, **23**, 9974–9989.
31 A. Beeby, I. M. Clarkson, R. S. Dickins, S. Faulkner, D. Parker, L. Royle, A. S. de Sousa, J. A. G. Williams and M. Woods, *J. Chem. Soc., Perkin Trans. 2*, 1999, 493–504.
32 I. R. Loftin, S. Franke, S. A. Roberts, A. Weichsel, A. Heroux, W. R. Montfort, C. Rensing and M. M. McEvoy, *Biochemistry*, 2005, **44**, 10533–10540.
33 Y. Xue, A. V. Davis, G. Balakrishnan, J. P. Stasser, B. M. Staehlin, P. Focia, T. G. Spiro, J. E. Penner-Hahn and T. V. O'Halloran, *Nat. Chem. Biol.*, 2008, **4**, 107–109.
34 E.-H. Kim, C. Rensing and M. M. McEvoy, *Nat. Prod. Rep.*, 2010, **27**, 711–719.
35 J. A. Delmar, C.-C. Su and E. W. Yu, *Biometals*, 2013, **26**, 593–607.
36 U. S. Raghavender, S. Aravinda, R. Rai, N. Shamala and P. Balaram, *Org. Biomol. Chem.*, 2010, **8**, 3133–3135.
37 H. Masuhara, H. Shioyama, T. Saito, K. Hamada, S. Yasoshima and N. Mataga, *J. Phys. Chem.*, 1984, **88**, 5868–5873.
38 M. Favre, K. Moehle, L. Jiang, B. Pfeiffer and J. A. Robinson, *J. Am. Chem. Soc.*, 1999, **121**, 2679–2685.
39 Z. Athanassiou, R. L. A. Dias, K. Moehle, N. Dobson, G. Varani and J. A. Robinson, *J. Am. Chem. Soc.*, 2004, **126**, 6906–6913.
40 R. L. A. Dias, R. Fasan, K. Moehle, A. Renard, D. Obrecht and J. A. Robinson, *J. Am. Chem. Soc.*, 2006, **128**, 2726–2732.
41 J. A. Robinson, *Acc. Chem. Res.*, 2008, **41**, 1278–1288.
42 O. Sénèque, E. Bourlès, V. Lebrun, E. Bonnet, P. Dumy and J.-M. Latour, *Angew. Chem., Int. Ed.*, 2008, **47**, 6888–6891.
43 O. Sénèque, E. Bonnet, F. L. Joumas and J.-M. Latour, *Chem.-Eur. J.*, 2009, **15**, 4798–4810.
44 A. Jacques, B. Mettra, V. Lebrun, J.-M. Latour and O. Sénèque, *Chem.-Eur. J.*, 2013, **19**, 3921–3931.
45 R. Czoik, A. Heintz, E. John and W. Marczak, *Acta Phys. Pol. A*, 2008, **114**, A51–A56.
46 G. Ramachandran, C. Ramakrishnan and V. Sasisekharan, *J. Mol. Biol.*, 1963, **7**, 95-.
47 S. A. Hollingsworth and P. A. Karplus, *Biomol. Concepts*, 2010, **1**, 271–283.
48 B. Bersch, K.-M. Derfoufi, F. De Angelis, V. Auquier, E. N. Ekende, M. Mergeay, J.-M. Ruysschaert and G. Vandenbussche, *Biochemistry*, 2011, **50**, 2194–2204.

